Ph.D. Dissertation of Chang Ki Yoon

Degeneration process of macular microstructure in retinitis pigmentosa

망막색소변성에서 황반부 망막 미세구조의 변성 과정

August 2022

Graduate School of Medicine
Seoul National University
Ophthalmology Major

Chang KI Yoon (윤창기)

Degeneration process of macular microstructure in retinitis pigmentosa

Name of Examiner

Submitting a Ph.D. Dissertation of
Chang Ki Yoon

April 2022

Graduate School of Medicine
Seoul National University
Ophthalmology Major

Chang Ki Yoon

Confirming the Ph.D. Dissertation written by
Chang Ki Yoon
July 2022

Chair _____(Seal)
Vice Chair _____(Seal)
Examiner _____(Seal)
Examiner _____(Seal)
Examiner _____(Seal)

Abstract

Keyword : retinitis pigmentosa; optical coherence tomography; retina; choroid; longitudinal studies

Student Number : 2014-30637

Purpose: To investigate the degeneration process in the retinal and choroidal microstructure of the macula in patients with retinitis pigmentosa (RP).

Methods: Spectral domain optical coherence tomography (SD-OCT) was analyzed in 177 RP patients and 177 healthy controls for cross sectional observation. The severity of RP was classified into three stages according to the integrity of the inner segment ellipsoid zone. Retinal nerve fiber layer (RNFL) and ganglion cell inner plexiform layer were manually segmented. These layer thickness was compared among moderate RP, advanced RP and control group. Pearson's correlation analyses were used to examine correlations between GCIPL thickness, RNFL thickness, visual acuity, and visual field extent in patients and controls. For longitudinal study, 69 patients with RP and same number of controls who underwent optical coherence tomography (OCT) over a 4-

year follow-up period were included. The retinal and choroidal layers were segmented manually from OCT images. The areas of retinal pigment epithelium (RPE) atrophy and choroidal vascular index (CVI) were also analyzed. Longitudinal changes of the OCT parameters were compared among the groups.

Results: GCIPL was significantly thicker in moderate than in control eyes ($P < 0.001$), but significantly thinner in advanced than in moderate eyes ($P < 0.001$) in both horizontal and vertical OCT scans. RNFL was significantly thicker in eyes with moderate and advanced than in controls in both horizontal and vertical meridians (all $P < 0.001$). GCIPL thickness showed a weak positive correlation with worse vision. RNFL thickness presented a weak positive correlation with worse vision and worse visual field extent. Longitudinal observation revealed that significant decreases (mean ± standard deviation in μm/year) in the thickness of the ganglion cell inner plexiform layer (GCIPL; −1.38±1.49), outer nuclear layer (ONL; −1.05±1.39), and inner segment ellipsoid (ISE; −0.93±0.71) at the moderate stage and retinal nerve fiber layer (RNFL; −1.46±1.11) and GCIPL (−0.94±1.54) at the advanced stage were observed. (all $P < 0.01$) Choroidal thickness decreased significantly from −7.62 to −9.40 um/year at all stages. RPE atrophy and CVI reduction were observed at the advanced stage. There was no change in the control.

Conclusion: Based on the cross-sectional analysis results, the inner

retina, including the GCIPL and RNFL, maintains its gross integrity longer than the photoreceptor layer in RP. Also, thickening of the inner retina may have some functional correlation in RP patients. In longitudinal observation, ONL and GCIPL thicknesses decreased at the moderate and advanced stages of RP, RNFL thickness decreased only at the advanced stage, and choroidal thickness decreased continuously. Additionally, RPE atrophy and CVI reduction were prominent at the advanced stage.

Table of Contents

List of Tables

List of Figures

Chapter 1. Introduction

1.1. Study Background

Retinitis pigmentosa (RP) is the most common and devastating inherited retinal disorder that eventually progresses to blindness. RP is caused by mutations in genes that play crucial roles in the photoreceptors and retinal pigment epithelium (RPE). [1]A pronounced early pathologic finding of RP is photoreceptor cell count reduction. [2] As human retinal specimens are difficult to obtain, histological studies are extremely limited. [3]Alternatively, rapid advances in imaging modalities, such as optical coherence tomography (OCT), have expanded insights into retinal microstructures in vivo. Indeed, understanding and interpreting the changes in macular microstructure is becoming more important to assess the remaining retinal structure and function in patients with RP. [4–7] The approach to restoration of vision should be tailored according to the level of structural damage. For example, the use of an artificial retina is feasible only if retinal ganglion cells are preserved at least. [8] Likewise, other treatment options that are currently under development require the integrity of certain macular structures, including the inner retina, RPE, and choroid, to be intact.

It is well known that the photoreceptor layer gradually thins and constricts as RP progresses and previous studies have shown that photoreceptor layer integrity, as evaluated by OCT, reflects

functional status in eyes with RP. [9-13] Postmortem morphometric studies have revealed that RP patients have lower photoreceptor and RGC counts, compared to normal controls. [3, 14] However, recent optical coherence tomography (OCT) studies indicated that the ganglion cell–inner plexiform layer (GCIPL) complex is preserved longer than the outer retinal (photoreceptor) layer. [5, 6] The macular RNFL changes are also unclear in RP patients. Some studies have shown RNFL thickening in RP patients, while others have shown RNFL thinning. [5, 6, 15] Additionally, the difference in choroidal thickness between patients with RP and healthy controls has been debated in several studies. [4, 7]

Currently most of studies about retinal structure are limited to cross–sectional observational study. However, the actual change of these structures in patients with RP could not be revealed robustly in the above–mentioned cross–sectional studies. Cross–sectional studies can be confounded by innate inter–individual variances rather than the pathologic process. A considerable variation in choroid thickness has been reported even among healthy subjects. [16] Therefore, longitudinal observation is required to assess degeneration of the retina and choroid in patients with RP. OCT is very useful to observe slowly progressing RP because OCT measurement is reliable and reproducible. [17]

1.2. Purpose of Research

The purpose of this study is to evaluate retinal and choroidal change in RP. First, inner retinal thickness of GCIPL and RNFL

within the macula in RP patients was evaluated using spectral domain OCT (SD-OCT) imaging through cross-sectional study. These data were compared among moderate, advanced and control group to figure out the difference as to disease severity. Also, the functional correlation with structural changes of the macular inner layers was analyzed including visual acuity and visual field defects. In order to find out the actual macular degeneration in patients with RP, longitudinal observation was performed. The thickness and structural changes in each layer of the retina and choroid were analyzed.

Chapter 2. Body

2.1. Methods

2.1.1. Participants

Patients diagnosed with RP at the hereditary retinal disease clinic of Seoul National University Hospital between 2009 and 2019 were enrolled in the present study. Only patients who were followed up for more than 42 months were included. Patients with a history of vitreoretinal surgery, glaucoma, and macular diseases such as epiretinal membrane and cystoid macular edema were excluded. Cataract was not excluded unless OCT signal strength is less than 6. History of cataract surgery before or after study enrollment was also not excluded. Epiretinal membrane was excluded if foveal pit was absent. We included the patients if retina was not stretched that foveal dimple is evident. [18] Cystoid macular edema was defined if more than five intraretinal cysts of any size exist with or without definite retinal thickening. Because central retinal thickness generally decreased in RP that macular edema can be underestimated. [19] We also excluded the case if CME developed during follow-up periods. Additionally, data of the same number of age-and sex-matched healthy controls were also collected.

Patients were divided into early, moderate, and advanced RP groups based on initial OCT findings. Constriction of remained ISE width is widely used to monitor progression of RP or evaluate the efficacy of treatment that severity grading based on ISE status can offer proper classification. The advanced and moderate groups were distinguished based on the visibility of the inner segment ellipsoid zone (ISE) on OCT images; the ISE was visible in the moderate group, but not in the advanced group. Advanced RP without any identifiable ISE but still having better vision than light perception alone. Patients with a significant peripheral visual field outside the central 20 degrees were excluded from the advanced group, because the OCT scan includes only the central visual field. The early group showed preserved ISE more than 2500 μm from the fovea, whereas the moderate group showed constricted ISE within 2500 μm from the fovea in OCT scans (Figure 1A).

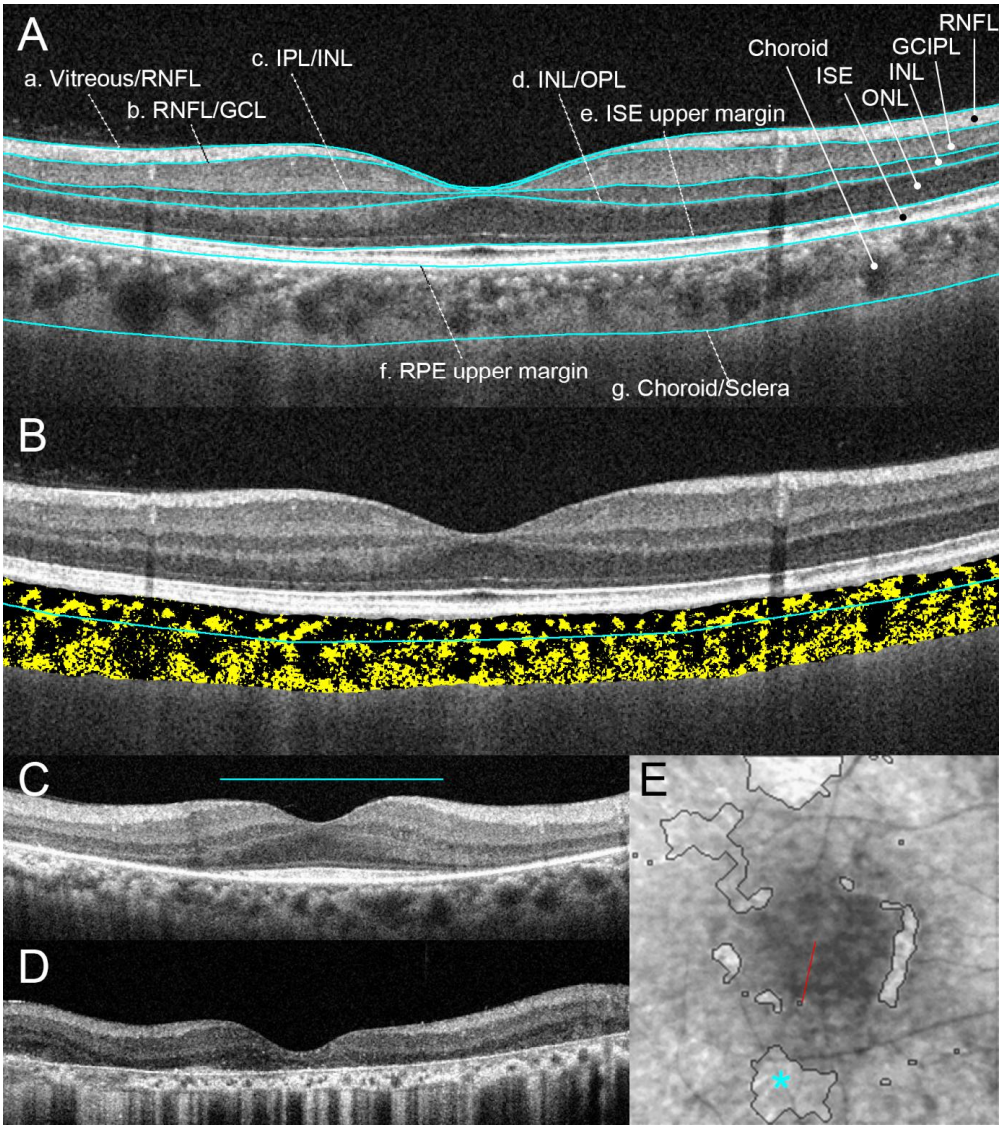

Figure 1. Representative examples of OCT analysis. (A) Manual segmentation of retinal layers. A case of early-stage RP. The ISE was preserved along the whole scan area. The blue line indicates the segmented border of the following: (a) the vitreous/RNFL, (b) the RNFL/GCL, (c) the IPL/INL, (d) the INL/OPL, (e) the upper margin of the ISE, (f) the upper margin of the RPE, and (g) the choroid/sclera. Each layer analysed is defined as following: RNFL: between (a) and (b); GCIPL: between (b) and (c); INL: between

(c) and (d); ONL: between (d) and (e); ISE: between (e) and (f); Choroid: between (f) and (g). (B) The choroid layer was binarized using the auto local threshold method using the same image as in (A) to calculate choroidal vascular index. The yellow pixel indicates the stromal region, and the dark pixel indicates the luminal region. (C) A case of moderate-stage RP. The ISE was preserved but was shorter than 6 mm of the whole scan width. The preserved ISE is marked with a blue line. (D) A case of advanced-stage RP. The ISE was not visible, and the OPL was also indiscernible. (E) Advanced RPE analysis shows the area of RPE atrophy, which is delineated with a black line. Blue asterisk indicates one of RPE atrophy area.
OCT, optical coherence tomography; RNFL, retinal nerve fiber layer; GCL, ganglion cell layer; IPL, inner plexiform layer; INL, inner nuclear layer; OPL, outer plexiform layer; ISE, inner segment ellipsoid zone; RP, retinitis pigmentosa

2.1.2. OCT acquisition and segmentation

Horizontal and vertical cross-sectional high-definition macular OCT scans were obtained using spectral-domain OCT (Cirrus 4000 HD OCT, Carl Zeiss Meditec, Inc., Dublin, CA, USA). Both horizontal and vertical image were used for cross-sectional analysis, and only vertical image was analyzed for longitudinal analysis. The right eye was selected for the analysis; however, if the right eye had severe media opacity or other diseases, the left eye was selected. The retinal and choroidal layers were segmented manually because the integrated segmentation algorithm of the OCT device is prone to errors in pathologic conditions. [20, 21] (Figure 1) The borders of the a) vitreous/RNFL, b) RNFL/ganglion cell layer (GCL), c) inner plexiform layer (IPL)/inner nuclear layer (INL), d) INL/outer plexiform layer (OPL), e) upper margin of the ISE, f) upper margin of the RPE, and g) choroid/sclera were manually delineated. The choroidal layer was subdivided into the inner and outer choroid, which contained mainly small/medium-sized and large choroidal vessels, respectively. [22, 23] Segmentation was performed by two masked graders. (Figure 2).

After manual segmentation, custom program developed in Python (Python Language Reference, version 3.6; The Python Software Foundation, Wilmington, DE, USA) measures the thickness of each allocated point as the distance from the fovea. The fovea was

marked manually at the most depressed point during manual segmentation. The average thickness of each layer within 2500 μm from the fovea was calculated. This is the same region where severity of RP was graded. RNFL is between a) and b), GCIPL is between b) and c), INL is between c) and d), ONL is between d) and e), ISE is between e) and f), choroid is between f) and g). Thickness is calculated as dividing the area by horizontal length.

For cross sectional analysis, RNFL and GCIPL thickness were used. And for longitudinal analysis, all the layers of initial and follow-up OCT scan were analyzed. The OCT image at the last follow-up visit was superimposed on the initial OCT image based on the RPE contour and fovea location using Photoshop CC (Adobe, San Jose, CA, USA). Thereafter, layer segmentation and thickness measurements were performed in the same manner as for the initial image. Segmentation data constructed by one grader were used for the analysis, after reliability of manual segmentation was confirmed by intraclass correlation coefficient (ICC)

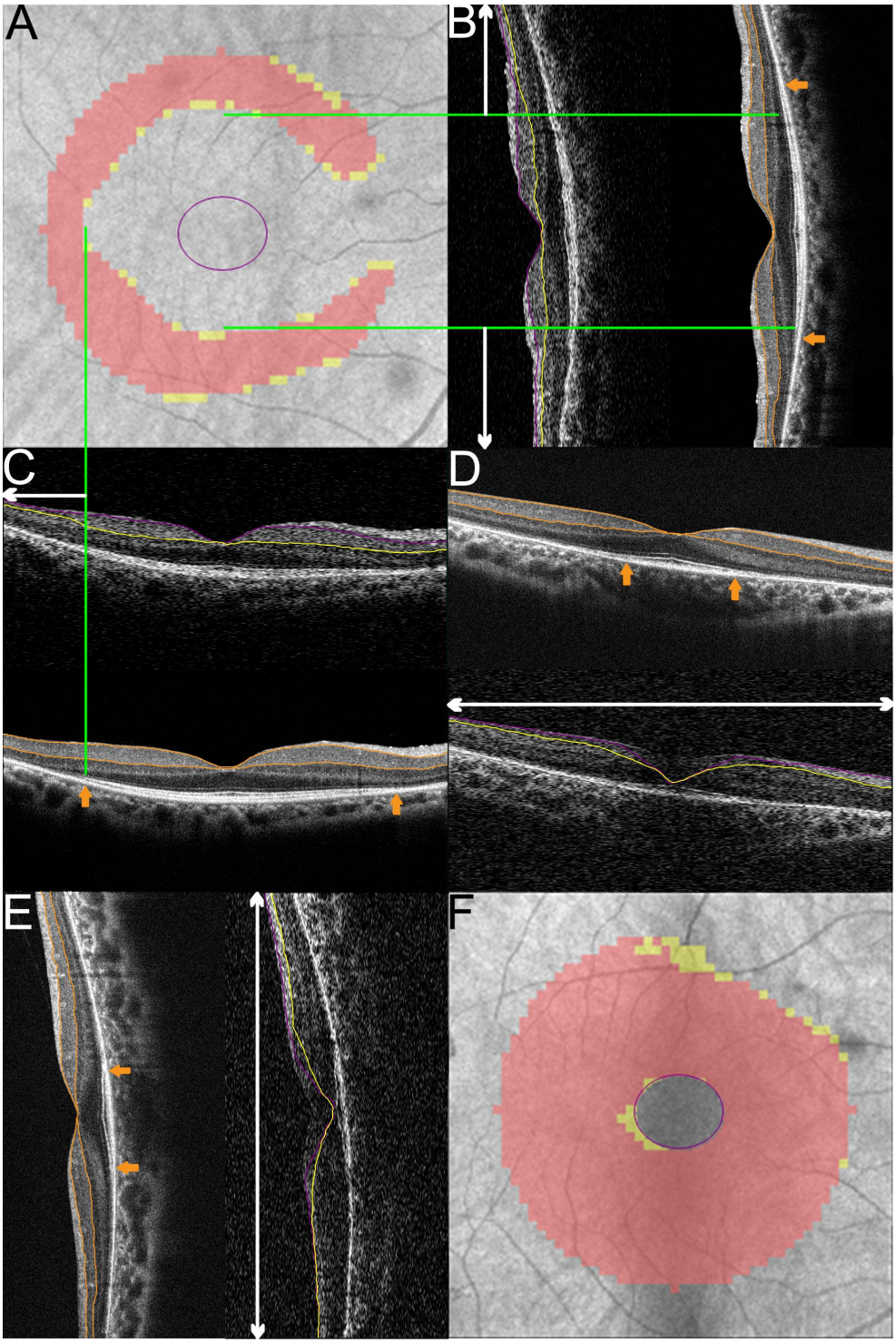

Figure 2. Errors in ganglion cell-inner plexiform layer (GCIPL) measurement rendered by the spectral domain optical coherence tomography (SD-OCT) built-in segmentation algorithm.

Segmentation errors are shown for two patients (A–C and D–F, respectively). Deviation maps (A and F) generated by the Cirrus OCT Ganglion Cell OU algorithm show comparisons of measured GCIPL thickness to normative data. Red and yellow areas indicate where the GCIPL is thinner than in 1% and 5% of normal eyes, respectively. The purple circle in the deviation map is the area where the Ganglion Cell OU algorithm could not be applied. Examples of GCIPL segmentation along the horizontal (C and D) and vertical (B and E) meridians are shown. The purple and yellow segmentation lines were automatically generated by Ganglion Cell OU segmentation algorithms. In comparison, the orange lines were manually generated and overlaid on the high-resolution scan. The preserved ISE length (distance between orange arrowheads) is longer in the first patient (A–C) than in the second patient (D–F). The segmentation errors (white arrows) were made largely because the embedded OCT algorithm mistook the retinal nerve fiber layer (RNFL) for the GCIPL. Further, the OCT algorithm made segmentation errors mostly where photoreceptor inner segments (ISE) were no longer visible (peripheral from the orange arrowheads) (B and C). As a result, these areas were labeled as abnormally thin in deviation maps (yellow and red areas of A and F). Green lines were made for comparing the location of ISE endpoint and the abnormally thinned area in the deviation map (A–C). Incorrect segmentation spanned nearly the entire scan of the second patient (D, E, and F), which was reflected in abnormal thinning over nearly the entire area of the deviation map (F).

2.1.3. Visual acuity and visual field

Goldmann kinetic perimetry was performed using a III4 target and the visual field was quantified, as previously described. [24] Using spherical coordinates, the surface area was computed and the subtended solid angle was calculated. This solid angle was represented as a percentage of the known mean visual field angle of normal controls (expressed in normalized solid angle units [nsu]). [24] For the statistical analyses, the visual acuity and visual field units were converted to logarithmic units. because they have geometric values, while arithmetic scales are required for the statistical analyses as correlation study.

2.1.4. RPE atrophy and Choroidal vascular index

The atrophic area of the RPE was measured using the Cirrus OCT software. The advanced RPE analysis program provides a sub-RPE illumination area where the light transmitted through the RPE is increased. RPE atrophy area was assessed through the sub-RPE illumination area in a 5-mm circle. [25] Niblack' s auto local thresholding was used to calculate choroidal vascular index (CVI). [26] The segmented choroidal layer was converted into an 8-bit grayscale format and binarized using the auto local threshold. The Scikit-image library of the Python language was used to perform this binarization. White pixels and dark pixels were considered the

stromal and luminal areas, respectively. CVI was defined as the proportion of the luminal area to the total choroidal area.

2.1.5. Statistics

For cross sectional analysis, comparisons between study groups of mean data were performed using unpaired t-tests, Pearson's chi-squared tests, the Mann-Whitney U test, and Fisher's exact test. A statistical package (SPSS Statistics 21.0 software, SPSS, Inc., Chicago, IL) was used to perform all statistical analyses and statistical significance was defined as $P < 0.05$. Data are expressed as mean ± standard deviation (SD).

For longitudinal observational study, comparisons of retinal thickness and visual acuity between the initial and last follow-up visits were performed using the Wilcoxon signed-rank test. Kruskal Wallis one-way ANOVA was performed to compare the baseline RPE and CVI difference among the three RP stages and Dunn post test was followed for multiple comparisons. Preserved ISE width is defined as horizontal length where ISE thickness is measurable. Pearson correlation analysis was done between ISE width and retinal layer thickness. Statistical analyses were performed using SPSS (version 25.0; IBM Corp, Armonk, NY, USA). This study adhered to the tenets of the Declaration of Helsinki, and the study protocol was approved by the institutional review board of Seoul National University Hospital (Approval no.: 1404-136-574).

2.2. Results

2.2.1. Cross sectional study

For cross sectional analysis, 476 retinitis pigmentosa patients received spectral domain OCT (SD-OCT) initially. Of these, 53 had an OCT signal strength of < 6. Sixty-four patients were unable to detect hand movement. The kinetic visual field was absent in 47 patients. The peripheral visual field was present in 56 patients. Vitreomacular traction and epiretinal membrane were detected in 143 patients. Cystoid macular edema was observed in 51 patients. Finally, 177 RP patients were included. The control groups were composed of healthy patients matched to the patients by age and gender. Gender was exactly matched, and age was matched within ± 3 years. Of 177 control patients, 90 were matched to the moderate group and 87 to the advanced group.

The advanced RP patients were significantly older than the moderate RP patients by 5 years Visual acuity and visual field were significantly better in the moderate patients than in the advanced patients (Snellen visual acuity: 20/29 in moderate and 20/1600 in advanced, $P < 0.001$; Visual field [normalized solid-angle units; nsu]: 3.94% in moderate and 1.73% in advanced, $P = 0.003$). Gender ratio and refractive error were not significantly different between any of the groups. This demographic data is shown in

Table 1.

Undetectable electroretinography (ERG) recordings were found in 56 out of 90 moderate patients (62.2%) and 58 out of 87 advanced patients (66.7%) for rod response; in 24 moderate patients (26.7%) and 41 advanced patients (47.1%) for maximal combined response; in 19 moderate patients (21.1%) and 42 advanced patients (48.3%) for cone response; and in 24 moderate patients (26.7%) and 35 advanced patients (40.2%) for 30 Hz flicker response. Undetectable maximal combined response and cone response were more frequent in advanced patients ($P = 0.008$ and < 0.001, respectively, chi-square test). The amplitude of all components was larger in moderate than advanced patients, but not significantly so (Table 1).

	Moderate control	Advanced control	Moderate RP	Advanced RP	P-value
Number of patients	90	87	90	87	
Age (years)	38.5 ± 12.9	45.3 ± 15.3	40 ± 14.8	45.1 ± 15.7	0.004 *
Male: Female	54:36	50:37	54:36	50:37	0.845 †
Spherical equivalent	−2.43 ± 1.94	−3.59 ± 3.55	−2.19 ± 2.99	−1.94 ± 3.07	0.855 *
Visual acuity (logMAR)			0.157 ± 1.19	1.903 ± 0.924	<0.001 *
Log Visual field (nsu)			0.596 ± 0.625	0.240 ± 0.800	0.003 *
Electroretinogram					
Rod response a wave			1.92 ± 3.47	0.99 ± 1.95	0.112 ‡
Rod response b wave			15.97 ± 32.92	8.39 ± 27.41	0.234 ‡
Maximal combined a wave			26.73 ± 38.04	20.43 ± 37.02	0.274 ‡
Maximal combined b wave			50.21 ± 82.25	35.02 ± 61.65	0.436 ‡
Cone response a wave			11.06 ± 10.21	6.28 ± 9.12	0.204 ‡
Cone response b wave			22.14 ± 24.75	11.92 ± 19.25	0.245 ‡
30-Hz flicker response			15.92 ± 19.13	10.98 ± 17.95	0.666 ‡
Inheritance pattern					0.011 §
Autosomal dominant			9 (10.0%)	12 (13.8%)	
Autosomal recessive			3 (3.3%)	9 (10.3%)	
Simplex			52 (57.8%)	29 (33.3%)	
X -linked			1 (1.1%)	1 (1.1%)	
Unknown			25 (27.8%)	36 (41.4%)	

Table 1 Demographics and ocular characteristics of control and retinitis pigmentosa (RP) patients.

Data are expressed as mean ± standard deviation.

* t-test between moderate and advanced group, † Pearson's Chi

square test between IISE and NISE, ‡ Mann–Whitney U test, and § Fisher’s exact test.

Moderate control and Advanced control mean control group of moderate RP and advanced RP, respectively

Nsu: normalized solid angle units

2.2.1.1. Ganglion Cell Inner Plexiform Layer Thickness Changes within the macula

There was good agreement between the two observers regarding GCIPL thickness evaluations. The mean ICC (ICC (95% confidence interval, P value)) was 0.951 (0.939 – 0.965, P < 0.001), 0.940 (0.915 – 0.953, P < 0.001) and 0.896 (0.887 – 0.908, P < 0.001) in each of the control, moderate RP, and advanced RP groups. The average GCIPL thickness along the horizontal meridian (70.9 ± 5.8 μm, 84.0 ± 10.0 μm, 71.2 ± 5.7 μm, and 78.1 ± 11.7 μm in the moderate control, moderate RP, advanced control, and advanced RP groups, respectively) was significantly higher in moderate and advanced RP groups compared to controls (both P < 0.001). The average GCIPL thickness along the vertical meridian (63.5 ± 5.2 μm, 71.7 ± 9.0 μm, 64.0 ± 5.1 μm, and 64.1 ± 10.0 μm in the moderate control, moderate RP, advanced control, and advanced RP groups, respectively) was significantly higher in moderate RP eyes than in control eyes (P < 0.001) but similar between advanced RP and control groups. Interestingly, the GCIPL thickness was lower in advanced RP eyes compared to moderate RP eyes in both the horizontal and vertical meridians (both P < 0.001) (Figure 3 A and B). The average GCIPL profiles are shown in Figure 4 A and B. For GCIPL thickness along horizontal meridian, difference was more apparent in temporal side than nasal side.

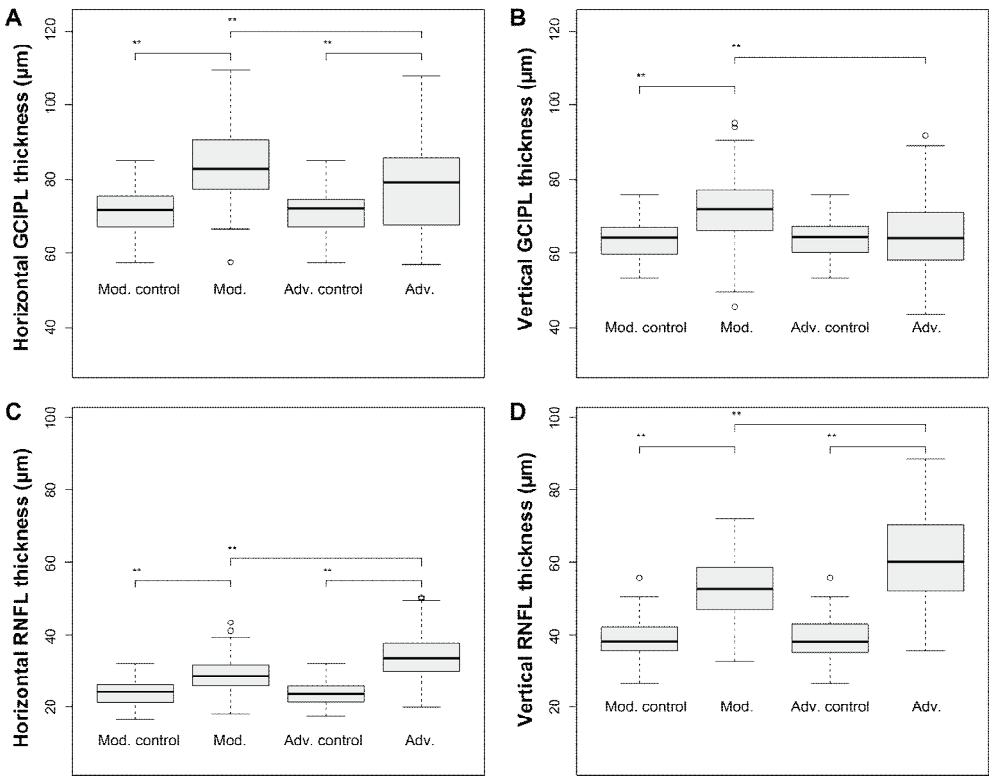

Figure 3. Box plots of average ganglion cell–inner plexiform layer (GCIPL) and retinal nerve fiber layer (RNFL) thickness in the moderate control, moderate, advanced control, and advanced along the horizontal (A, C) and vertical (B, D) meridians. The upper and lower margins of the box indicate the third and first quartiles, respectively, and the bold line (in the box) indicates the median. The upper horizontal bar indicates the value of third quartile plus 1.5 times the interquartile range [IQR] and the lower horizontal bar indicates the value of the first quartile minus 1.5 times the IQR. The open circles indicate data outliers. Asterisks (**) indicate a statistically significant difference between groups. The GCIPL thickness in moderate eyes was larger in moderate control along

either the horizontal or vertical meridians. However, the GCIPL thickness in advanced eyes was larger only along the horizontal meridian. The GCIPL was thinner in advanced than moderate eyes. Regarding RNFL thickness, it was larger in the moderate and advanced groups, compared to the respective control groups. The RNFL thickness was larger in advanced than moderate eyes. GCIPL and RNFL thickness were not significantly different between moderate and advanced controls. Note that advanced patients have more advanced retinitis pigmentosa compared to moderate patients.
Mod. : moderate; Adv: advanced

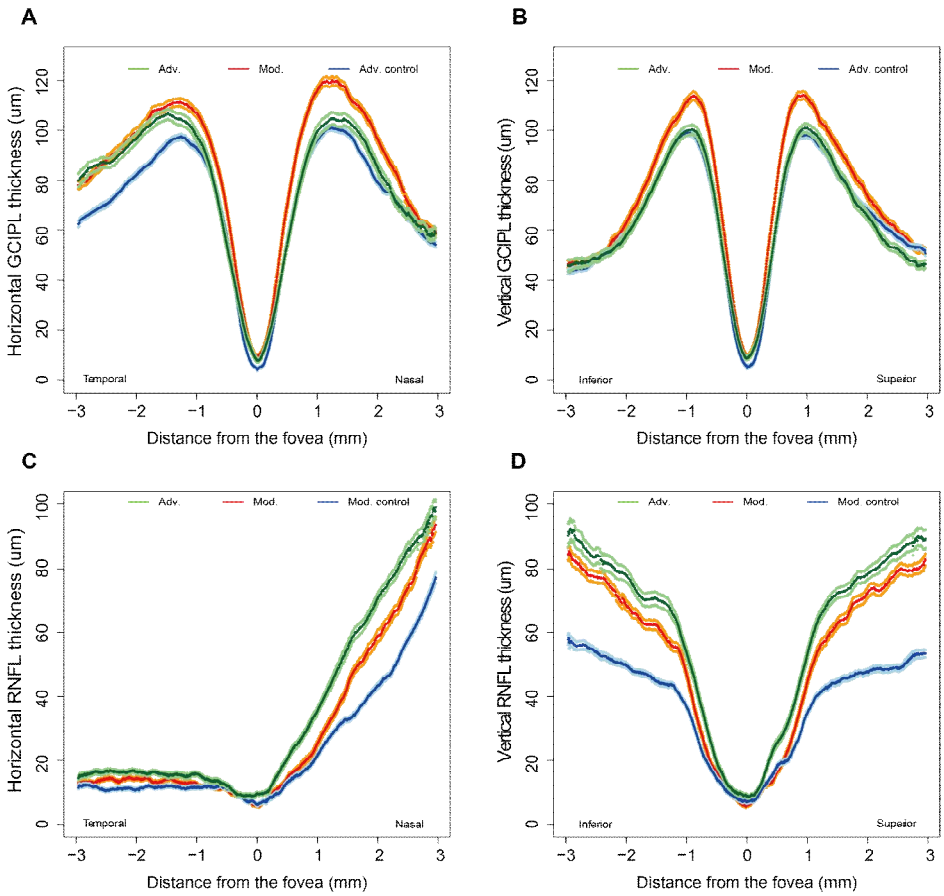

Figure 4. Horizontal and vertical ganglion cell-inner plexiform layer (GCIPL) and retinal nerve fiber layer (RNFL) thickness profiles. Mean data (Dark blue line, red line, dark green line) and ±1 SE (standard error) (light blue line, orange line, light green line) are shown. The GCIPL thickness is shown in the horizontal (A) and vertical (B) meridians. Profiles from advanced control patients are shown for comparison. moderate controls are not shown because they are similar to advanced controls, and the GCIPL thickness in moderate patients was much greater than that in advanced patients. In eyes with moderate RP, the GCIPL thickness was greater than that in the controls in all regions. In advanced RP eyes, the temporal

GCIPL was significantly thicker than in controls, but the nasal GCIPL was only slightly thicker. In the advanced group, the GCIPL thickness along the vertical meridian was similar to that of the advanced controls. The RNFL thickness profiles along the horizontal (C) and vertical (D) meridians are shown. The RNFL thickness of moderate and advanced eyes was larger than that in the controls in all regions, and larger in moderate than advanced eyes in all regions. advanced controls are not shown because they are similar to moderate controls, and the RNFL thickness in the advanced group was much larger than that in the moderate group. Note that advanced patients have more advanced retinitis pigmentosa than moderate patients.

Mod. : moderate; Adv: advanced

2.2.1.2. Retinal Nerve Fiber Layer Thickness Changes within the macula

Retinal Nerve Fiber Layer Thickness Changes within the macula

The high inter-observer agreement for RNFL thickness measurements were observed between the two observers. The ICC (ICC (95% confidence interval, P value)) was 0.942 (0.928 – 0.951, $P < 0.001$), 0.935 (0.915 – 0.942, $P < 0.001$) and 0.890 (0.878 – 0.912, $P < 0.001$) in each of the control, moderate RP, and advanced RP groups. The average RNFL thickness along the horizontal meridian (24.0 ± 3.3 μm, 28.9 ± 4.7 μm, 23.9 ± 3.2 μm, and 34.1 ± 6.6 μm in the moderate control, moderate RP, advanced control, and advanced RP groups, respectively) and the vertical meridian (38.8 ± 4.8 μm, 53.1 ± 8.2 μm, 38.9 ± 5.3 μm, and 61.0 ± 11.5 μm in the moderate-control, moderate RP, advanced-control, and advanced RP groups, respectively) was significantly higher in the moderate and advanced RP eyes than in the control eyes (all $P < 0.001$). Additionally, eyes with advanced RP had a significantly thicker RNFL than eyes with moderate RP along the horizontal and vertical meridians (both $P < 0.001$, Figure 3 C and D). The average RNFL profiles are shown in Figure 4 C and D. The RNFL thickness in moderate RP eyes was higher than in control eyes in all retinal quadrants examined (temporal, nasal, superior, and inferior). The RNFL in each of four quadrants was

also thicker in eyes with advanced RP than in eyes with moderate RP.

2.2.1.3. Relationship between the Ganglion Cell-Inner Plexiform Layer, the Retinal Nerve Fiber Layer, and Visual Function

Both logMAR visual acuity and the log−converted visual field extent were examined in the RP patients, but not in control groups. The GCIPL thickness was positively correlated with logMAR visual acuity in both the horizontal (R2 = 0.067, P = 0.012) and vertical (R2 = 0.065, P = 0.014) meridians. However, the GCIPL thickness was not associated with visual field extent in either the horizontal (R2 = 0.010, P = 0.210) or vertical (R2 = 0.010, P = 0.211) meridians.

In addition, a positive correlation was noted between the average RNFL thickness and logMAR visual acuity in both the horizontal (R2 = 0.098, P < 0.001) and vertical (R2 = 0.056, P = 0.002) meridians indicating positive correlation between thicker RNFL and worse vision. Moreover, the visual field extent was negatively correlated with average RNFL thickness in both the horizontal (R2 = 0.057, P = 0.003) and vertical (R2 = 0.030, P = 0.033) meridians. When we performed subgroup analysis (moderate and advanced), the significant correlation was observed only in the moderate group (Table 2).

	Both Moderate and Advanced		Moderate		Advanced	
	R^2	P	R^2	P	R^2	p
Hor. GCIPL vs VA	0.095	0.000*	0.068	0.012*	0.030	0.117
Ver. GCIPL vs VA	0.141	0.000*	0.066	0.014*	0.018	0.222
Hor. GCIPL vs VF	0.011	0.210	0.015	0.252	0.000	0.948
Ver. GCIPL vs VF	0.011	0.211	0.008	0.385	0.002	0.758
Hor. RNFL vs VA	0.099	0.000*	0.013	0.279	0.005	0.534
Ver. RNFL vs VA	0.056	0.002*	0.002	0.661	0.019	0.209
Hor. RNFL vs VF	0.057	0.003*	0.050	0.032*	0.009	0.499
Ver. RNFL vs VF	0.031	0.033*	0.019	0.194	0.002	0.773

Table 2. Relationship between the Ganglion Cell-Inner Plexiform Layer, the Retinal Nerve Fiber Layer, and Visual function

Hor. GCIPL: horizontal Ganglion Cell-Inner Plexiform Layer thickness; Ver. GCIPL: vertical Ganglion Cell-Inner Plexiform Layer thickness; Hor. RNFL: horizontal Retinal Nerve Fiber Layer thickness; Ver. RNFL: vertical Retinal Nerve Fiber Layer thickness; VA: visual acuity (logMar); VF: logarithm of Visual field represented as a percentage of the known mean visual field angle of normal controls (expressed in normalized solid angle units [nsu])

* Statistically significant P value ($P < 0.05$)

2.2.2. Longitudinal study

For longitudinal study, sixty-nine patients diagnosed with RP were finally included in the study. One case from moderate and 2 cases from advanced group was excluded because follow up OCT is not aligned well to the initial exam. The early, moderate, and advanced groups comprised 13, 17, and 39 patients, respectively.

Visual acuity decreased significantly during the follow-up period only in the advanced group. Age, sex and follow-up duration were not significantly different between the groups (Table 3). ICC analysis between independent graders was performed on retinal layer thickness measurement from 15 samples. Five cases were randomly selected from mild, moderate and advanced groups, respectively. All six retinal layers thickness of each sample were used. ICC (ICC (95% confidence interval, P value)) for RNFL, GCIPL, INL, ONL, ISE and choroid were 0.922 (0.900 – 0.933, $P < 0.001$), 0.931 (0.919 – 0.945, $P < 0.001$), 0.920 (0.911 – 0.929, $P < 0.001$), 0.919 (0.901 – 0.035, $P < 0.001$), 0.928 (0.911 – 0.940, $P < 0.001$) and 0.910 (0.899 – 0.922, $P < 0.001$). ICC for all retinal layers was excellent.

Group	Male:Female	Age (year)	Follow up (yr)	Initial VA	Follow-up VA	P-values†
Early	4:9	40.38 (14.08)	4.21 (1.12)	0.696 (0.476)	0.766 (0.551)	1
Moderate	9:8	35.76 (10.28)	4.29 (1.43)	0.608 (0.611)	0.533 (0.566)	0.555
Advanced	21:18	44.82 (14.79)	4.65 (1.41)	0.017 (0.150)	0.004 (0.121)	0.005*
Control	33.36	41.38 (14.03)	4.03 (1.28)	0.914 (0.745)	0.930 (0.694)	0.468
P value‡	0.372	0.189	0.405	< 0.001*	< 0.001*	

Table 3. Characteristics of patients at each stage of retinitis pigmentosa

Values are expressed as average (standard deviation)

VA: best-corrected visual acuity

†: the Wilcoxon signed-rank test between the initial and final visual acuity values, ‡: one-way ANOVA, *: P value less than 0.05

2.2.2.1. Retinal layer change

In the early and control groups, the retinal layer thickness did not change significantly between the initial and final examinations. In the moderate group, GCIPL, ONL, and ISE thickness (median [interquartile range]) decreased significantly over the follow-up period (78.6 ± 9.5 to 73.6 ± 8.7 μm, 83.4 ± 16.5 to 79.3 ± 19.0 μm, and 18.4 ± 9.9 to 14.7 ± 8.9 μm, respectively; p = 0.001, p = 0.005, and p <0.001, respectively; Wilcoxon's signed-rank test). In the advanced group, RNFL and GCIPL thickness decreased significantly over the follow-up period (53.0 ± 8.8 to 46.4 ± 7.7 μm and 69.0 ± 11.2 to 65.0 ± 10.3 μm, respectively; P <0.001 and P <0.001, respectively; Wilcoxon's signed-rank test). The thicknesses between the IPL and RPE in the advanced group remained unchanged. The changes in retinal layer thicknesses are summarized in Table 4 and Figure 5.

Group		RNFL	GCIPL	INL	ONL	ISE	IPL_RPE
Early	Change	−0.33 [−0.45 / 0.07]	0.21 [−0.52 / 1.06]	−0.08 [−0.73 / 0.70]	−0.48 [−0.72 / 0.05]	0.79 [−0.26 / 0.98]	
	P−value	0.168	0.542	0.946	0.14	0.146	
Moderate	Change	0.29 [−0.76 / 0.65]	−1.04 [−2.41 / −0.17]	0.11 [−0.19 / 0.63]	−1.44 [−1.86 / −0.28]	−0.74 [−1.33 / −0.49]	
	P−value	0.782	0.001*	0.378	0.005*	<0.001*	
Advanced	Change	−1.49 [−2.08 / −0.66]	−0.58 [−1.79 / 0.06]				−0.27 [−1.65 / 2.33]
	P−value	<0.001*	<0.001*				0.874
Control	Change	0.12 [−0.86 / 0.88]	−0.16 [−1.41 / 0.77]	−0.28 [−0.78 / 1.31]	0.36 [−1.47 / 1.20]	−0.14 [−1.94 / 1.27]	0.20 [−2.09 / 2.05]
	P−value	0.834	0.309	0.91	0.693	0.938	0.542

Table 4. Changes in the thickness of each retinal layer

Values are expressed as median [interquartile range]

Unit is ㎛/year

RNFL, retinal nerve fiber layer; GCIPL, ganglion cell inner plexiform layer; INL, inner nuclear layer; ONL: outer nuclear layer, ISE, inner segment ellipsoid zone; IPL_RPE: layer between inner plexiform layer and retinal pigment epithelium layer

*: P-value less than 0.05 (the Wilcoxon signed-rank test was performed between the initial and final thicknesses of each layer)

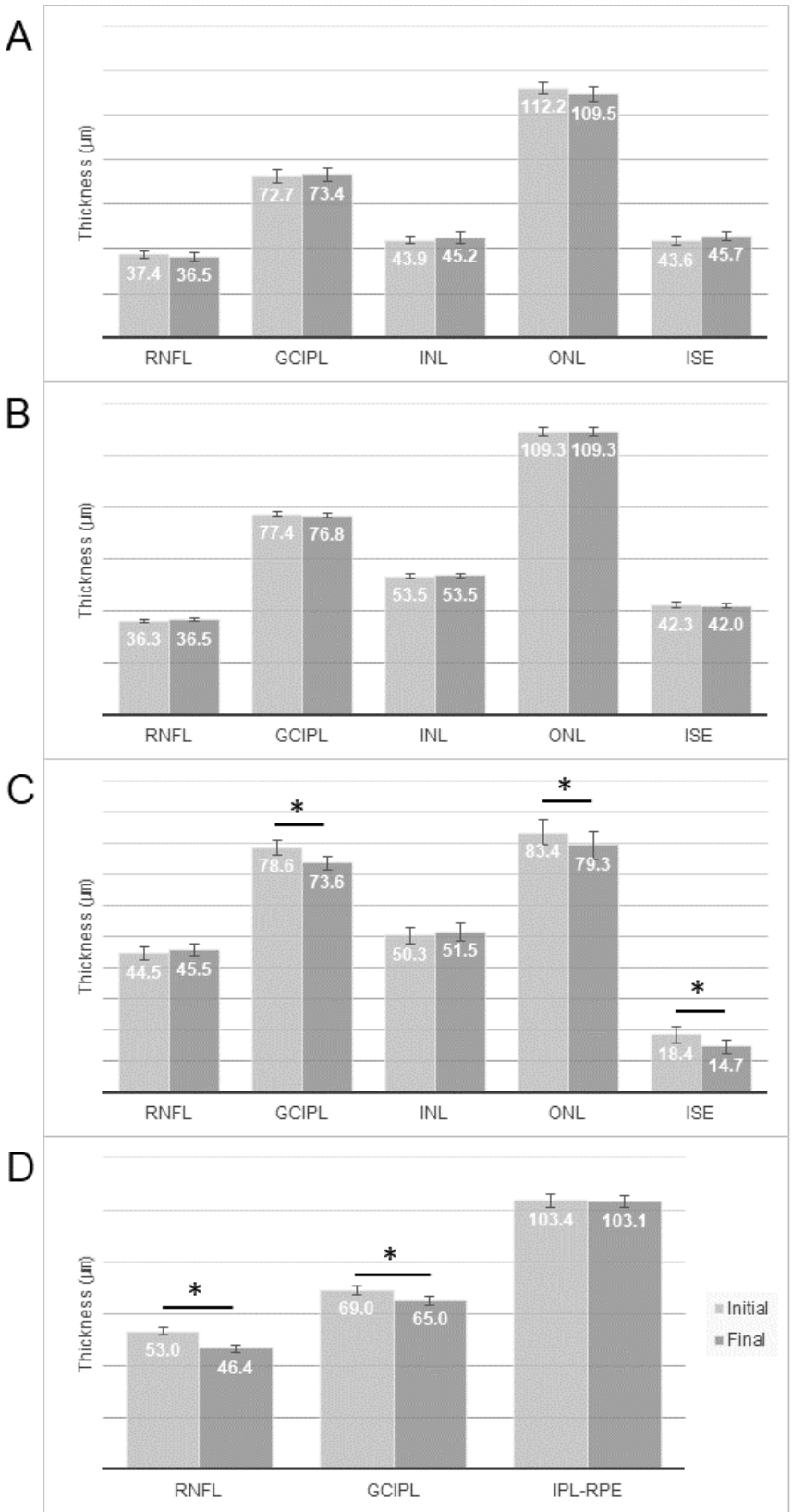
A
Thickness (μm)
37.4
36.5
72.7
73.4
43.9
45.2
112.2
109.5
43.6
45.7
RNFL
GCIPL
INL
ONL
ISE
B
Thickness (μm)
36.3
36.5
77.4
76.8
53.5
53.5
109.3
109.3
42.3
42.0
RNFL
GCIPL
INL
ONL
ISE
C
Thickness (μm)
*
*
*
44.5
45.5
78.6
73.6
50.3
51.5
83.4
79.3
18.4
14.7
RNFL
GCIPL
INL
ONL
ISE
D
Thickness (μm)
*
*
53.0
46.4
69.0
65.0
103.4
103.1
Initial
Final
RNFL
GCIPL
IPL-RPE

Figure 5. Change of retinal layer thickness in retinitis pigmentosa. The thickness of each layer at the initial and final visits is presented with an average value and error bar. (A) Healthy control group, (B) early group, (C) moderate group, and (D) advanced group. In the control and early groups, the retinal layer thickness did not change. In the moderate group, GCIPL, ONL, and ISE thicknesses decreased significantly over the follow-up period. In the advanced group, the RNFL and GCIPL thicknesses decreased significantly over the follow-up period.

RNFL, retinal nerve fiber layer; GCL, ganglion cell layer; INL, inner nuclear layer; ONL, outer nuclear layer; ISE, inner segment ellipsoid zone

* indicates $P < 0.05$, Wilcoxon's signed-rank test between the initial and final values

2.2.2.2. RPE and choroidal layer change

An increase of RPE atrophy area (average ± SD) was observed only in the moderate group (0.231 ± 0.607 to 1.390 ± 2.450 mm^2, P = 0.045, Wilcoxon's signed-rank test). Baseline RPE atrophy was significantly different between the groups (early, moderate, advanced, and control groups: 0.017 ± 0.058 mm^2, 0.231 ± 0.607 mm^2, 3.630 ± 3.280 mm^2, and 0.025 ± 0.074 mm^2, respectively; p <0.001, Kruskal Wallis test). A Dunn post test revealed that the baseline RPE atrophy area was significantly larger at the advanced stage than at the early, moderate, and control stages (P < 0.001 in all adjusted comparisons). There were no significant differences between the other groups. This result indicates that RPE atrophy was evident only at the advanced stage. Choroidal thickness decreased at all stages of RP (early, moderate, and advanced stages: 268.8 ± 52.4 to 240.5 ± 47.6 μm, 312.2 ± 48.0 to 286.3 ± 63.6 μm, and 266.0 ± 90.6 to 229.7 ± 88.6 μm, respectively) Both the inner and outer choroidal thicknesses simultaneously decreased. This change was significant, except for the inner choroid in the moderate group. The CVI did not change in any of the groups. However, the initial CVI was significantly lower at the advanced stage (67.31 ± 2.30, 67.07 ± 2.12, 59.17 ± 6.40, and 67.22 ± 2.73 in the early, moderate, advanced, and control groups, respectively; Kruskal Wallis test, P-value < 0.001;

Dunn posttest in control/advanced, early/advanced, and moderate/advanced, adjusted P-value < 0.01). The changes in choroidal-layer thicknesses, RPE atrophy area, and CVI are summarized in Table 5 and Figure 6. The retinal/choroidal layer thicknesses, RPE atrophy area, and CVI did not change significantly in healthy controls.

ISE width constriction is not correlated with retinal and choroidal thickness change. Initial ISE width showed positive relation to ONL thickness change, that means ONL thickness decreased faster as much as initial ISE width is small. (Table 6)

Group		RPE	Choroid	Cho_in	Cho_out	CVI
Early	Change	0 [0 / 0.02]	−4.55 [−7.18 / −2.43]	−2.71 [−3.61 / −0.15]	−2.28 [−3.94 / −1.46]	0.14 [−0.15 / 0.68]
	P−value	0.181	<0.001*	0.048*	0.021*	0.308
Moderate	Change	0.05 [0 / 0.40]	−11.75 [−14.30 / 1.93]	−2.08 [−3.56 / 0.13]	−6.12 [−11.47 / −0.59]	0.03 [−0.12 / 0.72]
	P−value	0.045*	0.01*	0.174	0.011*	0.193
Advanced	Change	0 [−0.42 / 0.41]	−7.95 [−16.09 / −3.92]	−2.86 [−5.09 / −0.94]	−5.19 [−10.48 / −1.60]	0.21 [−0.35 / 0.47]
	P−value	0.791	<0.001*	<0.001*	<0.001*	0.452
Control	Change	0 [0 / 0]	−2.13 [−6.72 / 5.06]	0.58 [−1.87 / 3.24]	−2.73 [−5.84 / 1.97]	−0.15 [−0.55 / 0.35]
	P−value	0.361	0.225	0.45	0.074	0.361

Table 5. Changes in the thickness of each choroidal layer, RPE atrophic area, and CVI

Unit is ㎟ for RPE atrophic area and ㎛/year for choroidal layer

RPE: retinal pigment epithelium; Cho_in: inner choroid; Cho_out: outer choroid; CVI: choroidal vascular index

*: P−value less than 0.05 (the Wilcoxon signed−rank test was performed between the initial and final values)

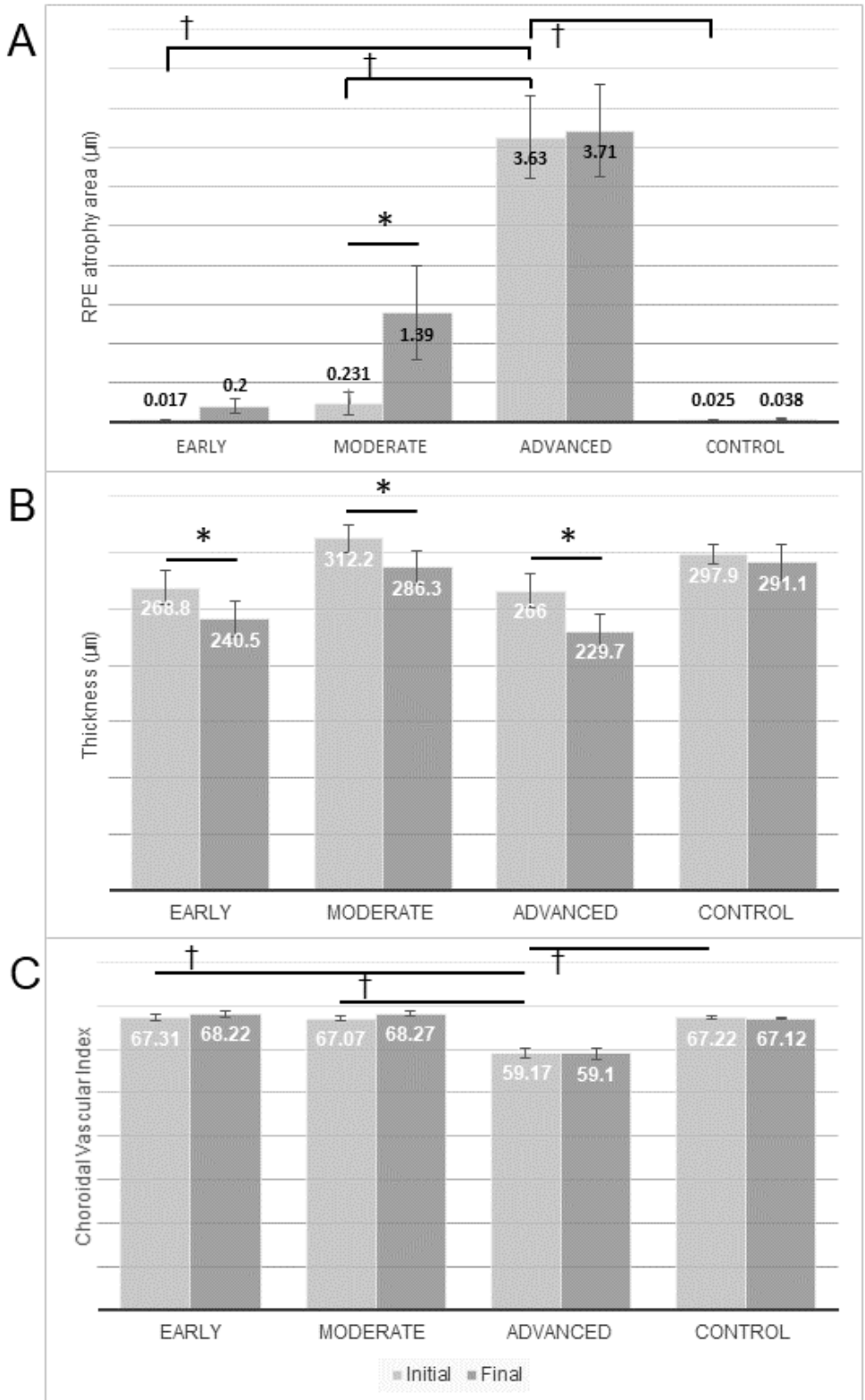
A
RPE atrophy area (μm)
0.017
0.2
0.231
1.39
3.63
3.71
0.025
0.038
EARLY
MODERATE
ADVANCED
CONTROL
B
Thickness (μm)
268.8
240.5
312.2
286.3
266
229.7
297.9
291.1
EARLY
MODERATE
ADVANCED
CONTROL
C
Choroidal Vascular Index
67.31
68.22
67.07
68.27
59.17
59.1
67.22
67.12
EARLY
MODERATE
ADVANCED
CONTROL
Initial
Final

Figure 6. Changes of retinal pigment epithelium (RPE) atrophy area, choroidal layer thickness, and choroidal vascular index (CVI) in retinitis pigmentosa. Values at the initial and final visits are presented with an error bar. (A) RPE atrophy area (mm^2) was assessed through the sub-RPE illumination area in a 5-mm circle. An increase of RPE atrophy area was observed only in the moderate group. Baseline RPE atrophy area was significantly different between the groups. ($P < 0.001$, Kruskal Wallis test). A Dunn post test revealed that the baseline RPE atrophy area was significantly larger at the advanced stage than at the early, moderate, and control stages ($P < 0.001$ in all adjusted comparisons of Dunn posttest). (B) Choroidal layer thickness decreased at all stages of RP but not in the control group. Initial choroidal layer thickness was not different among groups. Final choroidal layer thickness was different. Dunn post test revealed that only choroidal layer thickness of advanced stage was significantly smaller than that of control in multiple comparison. (Kruskal Wallis test, $P < 0.001$, Dunn posttest in advanced/control $P < 0.001$) (C) The CVI did not change in any of the groups. However, the initial CVI was significantly lower at the advanced stage. ($P < 0.001$ in Kruskal Wallis test, $P < 0.001$ in all adjusted comparisons of Dunn posttest)

* indicates $P < 0.05$, Wilcoxon's signed-rank test between the initial and final values

† indicates Dunn posttest adjusted $P < 0.001$

		RNFL	GCIPL	INL	ONL	Choroid	Cho_in	Cho_out	RPE	CVI
ISE width change	Correlation coefficient	−0.06	0.36	−0.34	−0.18	0.15	−0.01	0.19	0.04	−0.16
	P value	0.819	0.152	0.179	0.497	0.570	0.960	0.465	0.885	0.544
Initial ISE width	Correlation coefficient	0.47	0.05	−0.01	0.72	−0.4	−0.24	−0.39	−0.36	0.38
	P value	0.054	0.855	0.974	0.001*	0.111	0.350	0.127	0.230	0.147

Table 6. Correlation analysis between ISE width and retina/choroid layer thickness

RNFL, retinal nerve fiber layer; GCIPL, ganglion cell inner plexiform layer; INL, inner nuclear layer; ONL: outer nuclear layer, ISE, inner segment ellipsoid zone; Cho_in: inner choroid; Cho_out: outer choroid; RPE: retinal pigment epithelium atrophy area; CVI: choroidal vascular index

*: P−value less than 0.05 (Pearson correlation analysis)

2.3. Discussion

2.3.1. Cross-sectional study

This study demonstrates that the GCIPL and RNFL are preserved in both moderate and advanced RP patients. GCIPL was significantly thicker in eyes with moderate RP than in healthy eyes and advanced eyes. Also, eyes with moderate and advanced RP had a thicker macular RNFL than healthy eyes. To the best of our knowledge, this was the first description of GCIPL thickening within the macula in RP. This study included the larger number of RP subjects than previous similar OCT imaging studies. [5, 6, 27, 28]

Postmortem morphometric studies have revealed that retinal ganglion cells are relatively preserved compared to outer nuclear cells in eyes with RP. In previous studies which showed a significant reduction in the number of ganglion cells, the reduction was less profound than outer nuclear cell loss. [3, 14, 29] Studies in animal models of RP also support inner retinal preservation. Findings from an RP mouse model showed that retinal ganglion cells were resistant to degeneration, and that they retained their fine structures well after photoreceptor death. [30] Another study revealed inner nuclear layer (INL) and inner plexiform layer (IPL) thickening in a mouse model of Leber's congenital amaurosis (LCA). [31]

While pathologic study of RP patients is relatively lacking due to its

rarity, OCT images can provide detailed sectional images of the retina in situ. Several previous studies using OCT have shown that a generalized macular thickening develops in RP patients. Aleman et al. [27, 28] found inner retina thickening, along with outer nuclear layer loss, in eyes with RP caused by Rho (Rhodopsin) and RPGR (Retinitis pigmentosa GTPase regulator) mutations. Early-stage retinal thickening has also been reported in eyes with choroideremia. [32] However, these studies did not measure GCIPL thickness.

Several human studies suggested inner retinal thickening in RP patients. Thickening of the inner retinal layers, including the RNFL and the GCIPL, was detected on OCT images obtained from LCA patients. [31] In that study, time-domain OCT was used, so it was not possible to identify which layer had become thickened. However, the authors did show IPL thickening and Müller glial cell hypertrophy in a mouse model having the same mutation as human LCA patients. The authors suggested that Müller glial cell activation in neuronal injury may be responsible for IPL thickening. [33] Inner retinal thickening was also observed in less advanced RP patients, like those in our moderate group. [34] A detailed evaluation of the retinal layer was not performed in that study. Moreover, inner retinal layer thickening, especially of the inner nuclear layer, was observed in regions with outer nuclear layer thinning in RP patients having certain Rho mutations. [28]

Detailed retinal layer segmentation analyses using OCT images revealed controversial results on the GCIPL thickness in RP

patients. Hood et al. [5] observed that the average GCIPL thickness was similar between normal and RP eyes. Although the GCIPL on the temporal side was slightly thicker in RP eyes than in the controls in that study, the overall thickness was not significantly different, similar to our results of advanced RP. Vámos et al. [6] reported that GCIPL thickness was slightly larger when RP was less severe and a foveal mfERG signal was present, but no difference was statistically significant.

The pathogenesis of GCIPL thickening in eyes with RP is not clear. Neural remodeling may occur as the retina degenerates and may cause this thickening. [35, 36] It is known that vigorous retinal remodeling occurs after photoreceptor loss. Novel synapse formation from neural sprouting, microaneuroma formation, Müller cell hypertrophy, and amacrine and bipolar cell inversion are observed during remodeling phase 2 and 3. [35] All of these phenomena may contribute to GCIPL hypertrophy. The moderate RP patients in the current study might have had vigorous remodeling before GCIPL thickening. It was still difficult to separate the IPL from the GCIPL on the high-resolution SD-OCT images used in the current study. Therefore, our data on GCIPL thickening might have been influenced by IPL thickening caused by neural and/or glial remodeling. In addition to retinal remodeling, macular edema is likely to affect GCIPL thickness measurements. Although we excluded eyes with cystoid macular edema (CME) and definite cystoid spaces, subclinical non-cystoid macular edema may have contributed to GCIPL thickening. Fluorescein angiography can

reveal subtle macula edema and/or blood-retina barrier abnormalities. In support of this, previous studies have suggested that angiographic grading is correlated with OCT findings of CME in eyes with RP. [37, 38] Further study is needed to elucidate the pathogenesis of GCIPL thickening in eyes with RP.

Interestingly, we found that GCIPL thickness in the advanced RP group was less than that in the moderate RP group and nearly the same as in the normal control group. Looking at the normative data in our SD-OCT machine, macular GCIPL thickness decreased as age increased. Because our advanced group was older than the moderate group by an average of about 5 years, we created an age-matched normal control group to compare with the advanced group. Horizontal GCIPL and RNFL thickness were also greater in the advanced than in the controls. Because this was a cross-sectional study, inferences about GCIPL and RNFL thickness changes must be drawn cautiously. GCIPL thickness might increase at certain early stages of RP and decrease thereafter. We postulate that the GCIPL thickness reduction occurred because of neuronal atrophy that begins during neural remodeling. Postmortem investigations have shown that all types of retinal neurons decrease in advanced RP. Moreover, if GCIPL thickening results from edema, an inner retinal thinning would occur with edema resolution. However, in patients with more advanced RP than advanced patients, it is impossible to segment the neural retina using OCT scans. This may be because, in humans with advanced RP, the normal laminar organization of the neural retina is severely disrupted, with all of

the layers becoming intermingled. [39] Therefore, further observation of the GCIPL in eyes with more advanced RP is not possible with OCT.

We found that macular RNFL thickness was also increased in eyes with RP compared to normal controls. Unlike the GCIPL, the RNFL became thicker as RP advanced. This is in agreement with some previous studies examining RNFL thickness, [5, 6] but not all. Several groups have reported a relative thickening of the peripapillary RNFL, [5, 40] However, others have reported both thinning and thickening of the peripapillary RNFL. [15, 41–43] Glial tissue proliferation on the retinal surface has been suggested to cause this RNFL thickening. Altered metabolism of Muller cell from photoreceptor cell loss is known to morphologic transformation. Muller cell hypertrophy from during this transformation process can also render RNFL thickening. [44] Because we excluded patients who had an epiretinal membrane, this explanation does not apply to our observations. [6, 42] Although we excluded cases with epiretinal membrane, there may be substantial glial proliferation not obviously detected by OCT, [6, 43] Furthermore, glial cell proliferation within the RNFL or neuronal remodeling and migration into the RNFL can contribute to RNFL thickening. [5] Determining the actual mechanism of RNFL thickening in eyes with RP is beyond the scope of this study and further research is needed.

Both GCIPL and RNFL thickness profiles were created to examine if GCIPL and RNFL thicknesses change differently in each retinal location (Figure 4). We only observed topographical differences in

the GCIPL in the eyes of advanced patients. The temporal GCIPL maintained its thickness longer than the nasal, inferior, and superior retina (Figure 4). This relative GCIPL thickening pattern has also been observed previously. [5] In that study, mechanical expansion of the GCIPL to fill the empty space left by the degenerative photoreceptor layer was proposed. However, both GCIPL and RNFL thickness increased in moderate patients, in whom the photoreceptor layer was still relatively intact. Therefore, this mechanical stretch hypothesis cannot explain our results. However, it may be that neural remodeling or cone (or other neuron) density changes caused by RP have regional differences, resulting in varying thickness changes across the retina.

We generated a scatter plot comparing the retinal thickness and visual function to evaluate the trend of RNFL and GCIPL changes according to visual function deterioration. In the analysis of the entire RP group, GCIPL thickness was correlated with visual acuity, but not with the visual field. The GCIPL was thicker in patients whose visual acuity was relatively good. RNFL thickness was negatively correlated with visual acuity and visual field. These results are concordant with the GCIPL and RNFL thickness differences between subgroups. Horizontal GCIPL was thicker in the moderate eyes, and horizontal and vertical RNFL thickness were greater in the advanced eyes.

advanced and moderate categorization was based on an analysis of the inner segment ellipsoid zone shown in OCT. Visual acuity and visual field were worse in advanced eyes (Table 1). The ERG data,

undetectable rod response, and maximal combined response were more abundant in advanced eyes. These other examination results support the accuracy of the OCT-based grading system. These relationships were statistically significant because of the large number of subjects, even though the correlation coefficient was small. This might explain why only a few correlations were found in the subgroup analysis (Table 2).

Retinitis pigmentosa is an inherited disorder in which the progression and pattern are largely influenced by causal genetic variants. One limitation of this study was the lack of genotyping in the total study population. A difference in genotypes between our study groups might be a confounding factor. It is known that X-linked RP, having the RP2 and RPGR mutations, is usually associated with aggressive form of RP. Further studies including genotyping of the entire study population and long-term follow-up are required to elucidate how genetics might influence the morphologic changes associated with RP.

2.3.2. Longitudinal study

This study investigated the detailed changes in the retinal and choroidal structures within the macula over a 4-year-interval using a single OCT device. It can take several decades to progress from the early to advanced stages of RP. We included patients with RP of variable severities and defined their progression status based

on OCT features. This classification of severity and longitudinal observation can collaboratively extend our investigation to a much longer period than 4 years to the overview of the degeneration process in RP. ISE, ONL, and GCIPL thicknesses decreased at the moderate stage; GCIPL and RNFL thickness decreased at the advanced stage; and choroidal thickness decreased at all stages. In addition, baseline RPE atrophy was obvious at the advanced stage, while the RPE atrophy area increased significantly at the moderate stage. A decrease in CVI was observed only at the advanced stage. We summarized current finding and proposed the neurodegeneration process of the macula in Figure 7. Currently, this is based on limited number of patients and observation. Thus, this would be reliable if supported by further investigations.

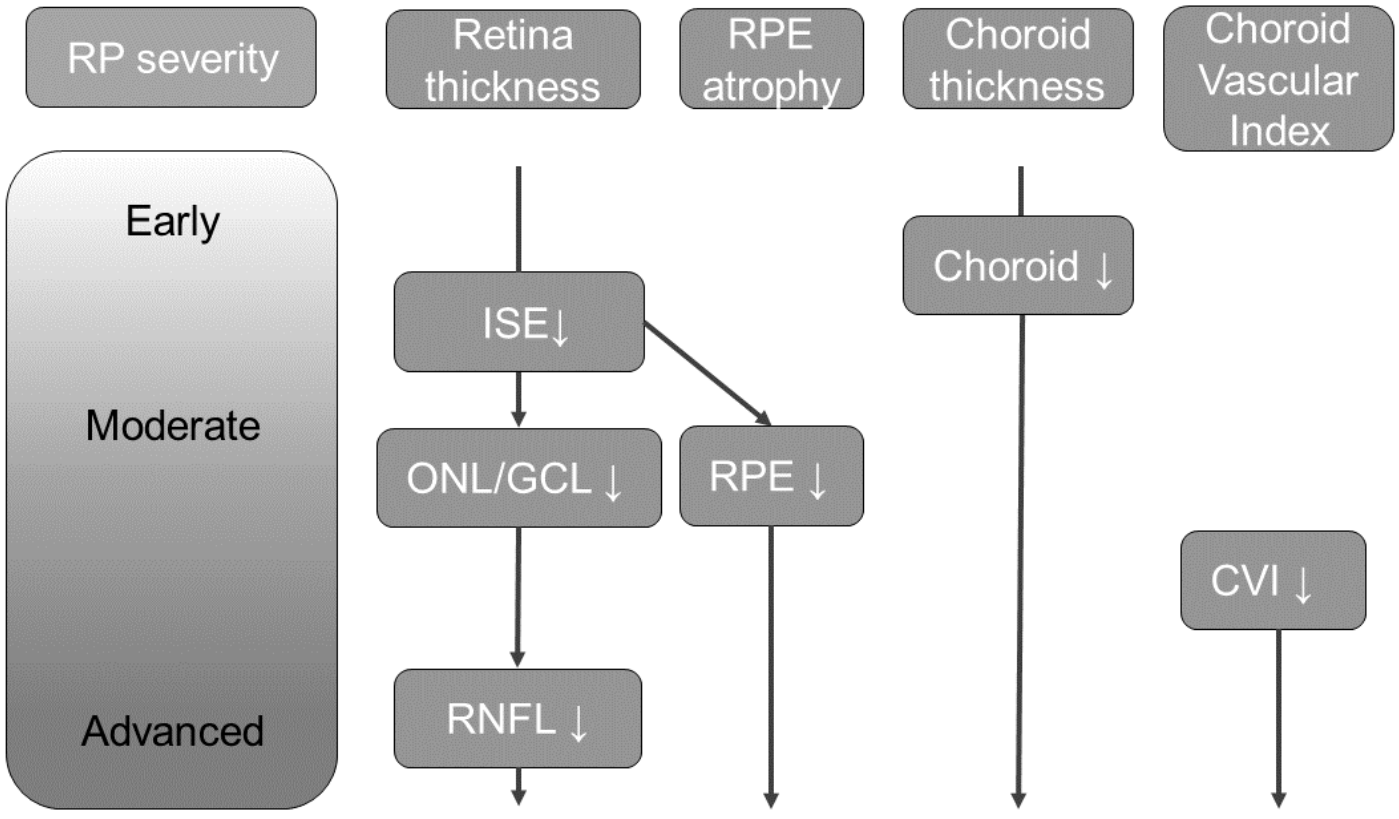
RP severity
Retina thickness
RPE atrophy
Choroid thickness
Choroid Vascular Index
Early
Moderate
Advanced
ISE↓
ONL/GCL ↓
RNFL ↓
RPE ↓
Choroid ↓
CVI ↓

Figure 7. Proposed retinal neurodegeneration process in retinitis pigmentosa. The ISE was degenerated earlier, followed by the ONL and GCL, and then the RNFL. Choroidal thickness decreased continuously from the early to the advanced stages, while RPE atrophy was observed after the moderate stage. CVI also decreased between the moderate and advanced stages.

ISE, inner segment ellipsoid zone; RNFL, retinal nerve fiber layer; GCL, ganglion cell layer; INL, inner nuclear layer; ONL, outer nuclear layer; RPE: retinal pigment epithelium; CVI: choroidal vascular index

The thinning of the retinal layer reflects retinal degeneration. ONL and GCIPL degeneration was observed at the moderate stage, and RNFL degeneration was present at the advanced stage. Notably, ISE degeneration appears to precede the moderate stage because the moderate group already had a constricted ISE. Most genetic alterations are associated with photoreceptor loss, and the earliest histologic change is photoreceptor cell count reduction. [1, 2] In the current study, ISE degeneration was also demonstrated as the earliest change. Trans-neuronal anterograde degeneration can explain the retinal degeneration process. [45] A decreased neuronal input from the photoreceptors can cause ganglion cell layer degeneration, and thereafter their axons start to degenerate, leading to RNFL thinning in the macula. In addition, OCT angiography has revealed attenuation of the inner retinal vasculature from the early stage of RP. [46] Vascular insufficiency may exacerbate or reflect inner retinal degeneration. This finding can support the concurrent thinning of the GCIPL and ONL observed in the current study. Correlation analysis in moderate stage revealed that initial ISE width is related to speed of ONL thickness decrease. It is supposed that ONL degeneration does not coincide with but follows after ISE degeneration.

The decrease of retinal layer thickness observed in the current study is consistent with the findings of the cross-sectional study. However, this study result could not find the increase of the RNFL and GCIPL thickness which observed in cross-sectional study. RNFL and GCIPL thickness increase observed in RP has also been

previously reported. [5, 6] This has been also observed in other disease. [47] Marc et al. suggested that neuronal remodeling contributes inner retinal thickening. [35] One possible hypothesis for this discrepancy is that the study duration of 4 years may not be sufficient to show GCIPL and RNFL thickness increase if the rate is much slower than the threshold of retinal thickness change can be detected in the current study design. Another explanation for GCIPL increase may develop before our early stage. Grading system used in current study is unable to differentiate the severity if preserved ISE margin is located outside OCT scan. Mid peripheral visual field defect or hypofluorescence in fundus autofluorescence photo were found in most of our early stage patients. Thus, GCIPL thickness increase cannot be found in current study if it occurs extremely earlier periode of RP.

Significant RPE atrophy was observed only at the baseline of the advanced stage, and the baseline RPE atrophy area was larger at the moderate stage than at the early stage, although the difference was not significant. Notably, a significant increase in RPE atrophy area was only found in the moderate group. These findings suggest that RPE atrophy of the macula commences at the moderate stage and is prominent at the advanced stage. This finding suggests that RPE atrophy occurs when photoreceptors are degenerated. This is supported by the findings of previous studies. A multimodal imaging study revealed that RPE cells migrate into the inner retina in response to photoreceptor cell degeneration. [48] RPE cells

detached from Bruch’ s membrane and migrated via the blood vessels into the inner retina in a human histopathologic study. [49] Regarding choroidal thickness, conflicting results exist in the literature. The majority of studies showed a decrease in choroidal thickness in patients with RP. [22, 50, 51] However, Tan et al. reported that the choroid was thicker in the RP group than in the control group. [7] In addition, the association between choroidal thickness and RP progression has not been well studied. One study showed that choroidal thickness did not differ according to RP severity and was inversely correlated with central foveal thickness. [51] Moreover, regarding the subdivided choroidal layer, one study showed that the outer choroid layer, which comprises relatively larger vessels, was smaller in patients with RP than in controls. [4] The current longitudinal study clarified that choroidal thickness continuously decreased at any stage of RP. Baseline average choroidal thickness of moderate group is greater than even that of control group in current study. This seems to be inconsistent with continuous decrease of choroidal thickness in RP. However, the difference is not statistically significant. (Kruskal Wallis test, P = 0.398) And choroidal thickness is reported to vary greatly even among healthy adults. [16, 52] Refractive error or age are reported to be associated with choroidal thickness in those studies. Current study did not control these factors. Therefore, longitudinal change investigation can be more reliable and should be emphasized than cross sectional comparison in evaluating choroidal thickness. This study also showed a simultaneous reduction of inner and outer

choroidal layer thicknesses. Choroidal vascularity analysis results in RP, assessed using the CVI, have been debated. CVI was reported to decline in patients with RP in several studies. [4, 53] However, Murakami et al. showed that CVI did not differ regardless of the presence or severity of RP. [51] In the current study, CVI was stable in both RP and control groups, but the baseline CVI was significantly lower in the advanced RP group. This finding, along with a decrease in choroidal thickness, suggests that the luminal and stromal areas decreased by the same proportion until the moderate stage. Subsequently, the luminal area is likely to degenerate faster than the stromal area at the advanced stage of RP. Kawano et al. showed that the luminal area decreased relatively more than the stromal area, where retinal degeneration was evident. [53] This finding is consistent with our finding that CVI reduction occurred between the moderate and advanced stages. Moreover, CVI has been shown to be correlated with choroidal blood flow and a decrease in choroidal blood flow has been reported in patients with RP. [51, 54] The current CVI data suggest that choroidal blood flow might remain stable until the moderate stage and reduce between the moderate and advanced stages.

Several hypotheses regarding choroidal thickness changes in RP have been suggested. A decrease in choroidal thickness can occur secondary to retinal degeneration and a decreased demand for oxygen and nutrients. [55] Additionally, RPE cell loss can lead to choroidal vessel atrophy. [56, 57] A decrease in trophic factors due to RPE degeneration could lead to choroidal thinning. [58] For

example, vascular endothelial growth factor (VEGF) A, which maintains the choriocapillaris, is proposed as a principal mediator that decreases and renders choroidal thinning. [4] Intraocular VEGF level was reported to be lower in patients with RP. [59] Notably, the current study revealed that choroidal thickness decreased even at the early stage when the overlying retina and RPE were intact. Thus, choroidal thickness reduction seems to be affected by definite degeneration of the remote peripheral retina or generalized degeneration of the photoreceptor, although it is not observed on OCT. This differs from pattern of retinal degeneration, which is closely related to the adjacent retinal layer integrity. The choroid is not bound by the neuronal circuit to the retina but is supposed to crosstalk with the retina via other factors, such as cytokines or trophic factors. At the early stage, an obvious outer retinal loss was observed outside the macula, especially at the mid-periphery. However, photoreceptors lose their function in the whole retina, which is evidenced by the decrease or extinction of ERG activity even at the early stage. Metabolic demand from the photoreceptors is likely to maintain the stroma and vascular tone through unknown trophic factors or signals. Thus, overall photoreceptor degeneration of whole retina at an early stage is likely to result in choroid thickness reduction.

The degeneration process of the retina and choroid proposed in this study may suggest an effective treatment window for RP. Cell therapy, gene augmentation therapy, gene editing therapy, optogenetic therapy, and artificial retinal prostheses require

functioning retinal structures other than photoreceptor cells. The current study suggests that RP treatment can be effective, at least at the moderate stage, when the inner retina, RPE, and choroidal circulation are not substantially impaired. This study can also help select optimal excitatory targets for artificial retina or optogenetic treatments according to the patients' stage of retinal degeneration. The present study had several limitations. First, eye tracking was not implemented in the OCT follow-up. Alternatively, we aligned the follow-up images manually using the OCT fundus image marked with the scan location and excluded cases with unmatched follow-up OCT images. Subsequently, by superimposing the follow-up OCT image on the initial image, tilting and fovea centering were finely tuned for matching. Second, the choroidal structure was analyzed using structural OCT rather than OCT angiography. The choroidal vasculature change is expected to be more accurately elucidated using OCT angiography, and analysis using OCT angiography should be performed in a future study. Third, genetic diagnosis was performed in limited cases. Sequencing was done in 17 cases and possible causal variant was identified in 9 cases. (Table 7) Our cohort comprised unrelated individuals enrolled from a single center. We analyzed the genetic diagnosis of RP and found that the prevalence of causal genes was consistent with that reported by other groups. Therefore, the results of the present study are unlikely to be biased by a specific genetic background. Further longitudinal observations of genetically confirmed patients

are needed to reveal genotype-phenotype relation on macular structure change.

Identifier	Inheritance	Gene name	Zygosity	Nucleotide	Amino acid	Zygosity	Nucleotide	Amino acid
RPL_1	AR	*USH2A*	het	c.14287G>A	p.Gly4763Arg	het	c.1190T>A	p.Ile397Lys
RPL_11	AR	*NMNAT1*	het	c.A701G	p.Q234R	het	c.C709T	p.R237C
RPL_12	Sporadic	*C2ORF71*	het	c.2008dupC	p.Leu670fs	het	c.878T>C	p.Leu293Pro
RPL_14	AD	*PRPF31*	het	c.421−1G>A				
RPL_15	AD	*RP1*	het	c.2184delG	E728fs			
RPL_3	Sporadic	*EYS*	het	c.8868C>A	p.Tyr2956*	het	c.525_527delGGA	
RPL_8	AR	*USH2A*	het	c.8559−2A>G		het	c.A6485T	p.Q2162L

Table 7 Possible disease causing variant revealed in this study participants

AR: autosomal recessive; AD: autosomal dominant; het: heterozygote

Chapter 3. Conclusion

GCIPL and RNFL were preserved based on SD-OCT in this study with a large patient cohort. The GCIPL was thicker in eyes with moderate RP, but decreased to near-normal values in advanced RP, which indicates that the ganglion cell layer maintains its volume in advanced patients who have less than 5/200 vision or less than a 5' visual field. Therefore, we might anticipate that implanted cells and microchip devices have the potential to provide vision in advanced RP patients with loss of photoreceptor layer.

Moreover, longitudinal study determined that the retina degenerated in the order of ISE, ONL/GCIPL, and RNFL in eyes with RP using OCT. Also, we found that reduced CVI and RPE atrophy were observed only at the advanced stage. This finding supports the concept that the primary site of degeneration in RP is the outer segment of the photoreceptor, followed by photoreceptor cell bodies and ganglion cells. Prominent and continuous thinning of the choroid from the early stage is an interesting finding, but the exact pathological mechanism underlying the choroidal thinning needs to be further elucidated in future studies. Our findings on retinal and choroidal degeneration could guide future regenerative treatments in terms of precision medicine.

Bibliography

1. Verbakel SK, van Huet RAC, Boon CJF, den Hollander AI, Collin RWJ, Klaver CCW, Hoyng CB, Roepman R, Klevering BJ (2018) Non-syndromic retinitis pigmentosa. Prog Retin Eye Res 66:157–186
2. Milam AH, Li ZY, Fariss RN (1998) Histopathology of the human retina in retinitis pigmentosa. Prog Retin Eye Res 17:175–205
3. Santos A, Humayun MS, de Juan Jr. E, Greenburg RJ, Marsh MJ, Klock IB, Milam AH (1997) Preservation of the inner retina in retinitis pigmentosa. A morphometric analysis. Arch Ophthalmol 115:511–515
4. Egawa M, Egawa M, Mitamura Y, et al (2019) Correlations between choroidal structures and visual functions in eyes with retinitis pigmentosa. Retina 39:2399–2409
5. Hood DC, Lin CE, Lazow MA, Locke KG, Zhang X, Birch DG (2009) Thickness of receptor and post-receptor retinal layers in patients with retinitis pigmentosa measured with frequency-domain optical coherence tomography. Invest Ophthalmol Vis Sci 50:2328–2336
6. Vamos R, Tatrai E, Nemeth J, Holder GE, DeBuc DC, Somfai GM (2011) The structure and function of the macula in patients with advanced retinitis pigmentosa. Invest Ophthalmol Vis Sci 52:8425–8432
7. Tan R, Agrawal R, Taduru S, Gupta A, Vupparaboina K, Chhablani J (2018) Choroidal vascularity index in retinitis pigmentosa: An OCT study. Ophthalmic Surg Lasers Imaging Retin 49:191–197
8. Chader GJ, Weiland J, Humayun MS (2009) Artificial vision: needs, functioning, and testing of a retinal electronic prosthesis. Prog Brain Res 175:317–332
9. Birch DG, Locke KGI, Wen Y, Locke KGI, Hoffman DR, Hood DC (2013) Spectral-domain optical coherence tomography measures of outer segment layer progression in patients with X-linked retinitis pigmentosa. JAMA Ophthalmol 131:1143–1150
10. Fischer MD, Fleischhauer JC, Gillies MC, Sutter FK, Helbig H, Barthelmes D (2008) A New Method to Monitor Visual Field Defects Caused by Photoreceptor Degeneration by

Quantitative Optical Coherence Tomography. Investig Opthalmology Vis Sci 49:3617
11. Sugita T, Kondo M, Piao CH, Ito Y, Terasaki H (2008) Correlation between macular volume and focal macular electroretinogram in patients with retinitis pigmentosa. Invest Ophthalmol Vis Sci 49:3551–3558
12. Rangaswamy N V, Patel HM, Locke KG, Hood DC, Birch DG (2010) A comparison of visual field sensitivity to photoreceptor thickness in retinitis pigmentosa. Invest Ophthalmol Vis Sci 51:4213–4219
13. Yoon CK, Yu HG (2013) The Structure–Function Relationship between Macular Morphology and Visual Function Analyzed by Optical Coherence Tomography in Retinitis Pigmentosa. J Ophthalmol 2013:821460
14. Stone JL, Barlow WE, Humayun MS, de Juan Jr. E, Milam AH (1992) Morphometric analysis of macular photoreceptors and ganglion cells in retinas with retinitis pigmentosa. Arch Ophthalmol 110:1634–1639
15. Anastasakis A, Genead MA, McAnany JJ, Fishman GA (2012) Evaluation of retinal nerve fiber layer thickness in patients with retinitis pigmentosa using spectral–domain optical coherence tomography. Retina 32:358–363
16. Tan CSH, Cheong KX (2014) Macular Choroidal Thicknesses in Healthy Adults—Relationship With Ocular and Demographic Factors. Invest Ophthalmol Vis Sci 55:6452–6458
17. Sala–Puigdollers A, Figueras–Roca M, Hereu M, Hernández T, Morató M, Adán A, Zarranz–Ventura J (2018) Repeatability and reproducibility of retinal and choroidal thickness measurements in Diabetic Macular Edema using Swept–source Optical Coherence Tomography. PLoS One 13:e0200819
18. Govetto A, Lalane RA, Sarraf D, Figueroa MS, Hubschman JP (2017) Insights Into Epiretinal Membranes: Presence of Ectopic Inner Foveal Layers and a New Optical Coherence Tomography Staging Scheme. Am J Ophthalmol 175:99–113
19. Gorovoy IR, Gallagher DS, Eller AW, Mayercik VA, Friberg TR, Schuman JS (2013) Cystoid macular edema in retinitis pigmentosa patients without associated macular thickening. Semin Ophthalmol 28:79–83
20. Bahrami B, Ewe SYP, Hong T, Zhu M, Ong G, Luo K, Chang A (2017) Influence of Retinal Pathology on the Reliability of Macular Thickness Measurement: A Comparison Between Optical Coherence Tomography Devices. Ophthalmic Surgery,

Lasers Imaging Retin 48:319–325
21. Garas A, Papp A, Hollo G (2013) Influence of age−related macular degeneration on macular thickness measurement made with fourier−domain optical coherence tomography. J Glaucoma 22:195–200
22. Adhi M, Regatieri C V, Branchini LA, Zhang JY, Alwassia AA, Duker JS (2013) Analysis of the morphology and vascular layers of the choroid in retinitis pigmentosa using spectral−domain OCT. Ophthalmic Surg Lasers Imaging Retin 44:252–259
23. Sim DA, Keane PA, Mehta H, Fung S, Zarranz−Ventura J, Fruttiger M, Patel PJ, Egan CA, Tufail A (2013) Repeatability and reproducibility of choroidal vessel layer measurements in diabetic retinopathy using enhanced depth optical coherence tomography. Investig Ophthalmol Vis Sci 54:2893–2901
24. Jacobson SG, Yagasaki K, Feuer WJ, Roman AJ (1989) Interocular asymmetry of visual function in heterozygotes of X−linked retinitis pigmentosa. Exp Eye Res 48:679–691
25. Hariri A, Nittala MG, Sadda SR (2015) Outer retinal tubulation as a predictor of the enlargement amount of geographic atrophy in age−related macular degeneration. Ophthalmology 122:407–413
26. Pellegrini M, Bernabei F, Mercanti A, Sebastiani S, Peiretti E, Iovino C, Casini G, Loiudice P, Scorcia V, Giannaccare G (2020) Short−term choroidal vascular changes after aflibercept therapy for neovascular age−related macular degeneration. Graefe's Arch Clin Exp Ophthalmol. https://doi.org/10.1007/s00417−020−04957−5
27. Aleman TS, Cideciyan A V, Sumaroka A, et al (2007) Inner retinal abnormalities in X−linked retinitis pigmentosa with RPGR mutations. Invest Ophthalmol Vis Sci 48:4759–4765
28. Aleman TS, Cideciyan A V, Sumaroka A, et al (2008) Retinal laminar architecture in human retinitis pigmentosa caused by Rhodopsin gene mutations. Invest Ophthalmol Vis Sci 49:1580–1590
29. Humayun MS, Prince M, de Juan Jr. E, Barron Y, Moskowitz M, Klock IB, Milam AH (1999) Morphometric analysis of the extramacular retina from postmortem eyes with retinitis pigmentosa. Invest Ophthalmol Vis Sci 40:143–148
30. Lin B, Peng EB (2013) Retinal ganglion cells are resistant to photoreceptor loss in retinal degeneration. PLoS One 8:e68084
31. Cideciyan A V, Aleman TS, Jacobson SG, et al (2007)

Centrosomal–ciliary gene CEP290/NPHP6 mutations result in blindness with unexpected sparing of photoreceptors and visual brain: implications for therapy of Leber congenital amaurosis. Hum Mutat 28:1074–1083
32. Jacobson SG, Cideciyan A V, Sumaroka A, Aleman TS, Schwartz SB, Windsor EA, Roman AJ, Stone EM, MacDonald IM (2006) Remodeling of the human retina in choroideremia: rab escort protein 1 (REP–1) mutations. Invest Ophthalmol Vis Sci 47:4113–4120
33. Rattner A, Nathans J (2005) The genomic response to retinal disease and injury: evidence for endothelin signaling from photoreceptors to glia. J Neurosci 25:4540–4549
34. Wolsley CJ, Silvestri G, O'Neill J, Saunders KJ, Anderson RS (2009) The association between multifocal electroretinograms and OCT retinal thickness in retinitis pigmentosa patients with good visual acuity. Eye 23:1524–1531
35. Marc RE, Jones BW, Watt CB, Strettoi E (2003) Neural remodeling in retinal degeneration. Prog Retin Eye Res 22:607–655
36. Fisher SK, Lewis GP, Linberg KA, Verardo MR (2005) Cellular remodeling in mammalian retina: results from studies of experimental retinal detachment. Prog Retin Eye Res 24:395–431
37. Hirakawa H, Iijima H, Gohdo T, Tsukahara S (1999) Optical coherence tomography of cystoid macular edema associated with retinitis pigmentosa. Am J Ophthalmol 128:185–191
38. Chung H, Hwang JU, Kim JG, Yoon YH (2006) Optical coherence tomography in the diagnosis and monitoring of cystoid macular edema in patients with retinitis pigmentosa. Retina 26:922–927
39. Jones BW, Watt CB, Frederick JM, Baehr W, Chen CK, Levine EM, Milam AH, Lavail MM, Marc RE (2003) Retinal remodeling triggered by photoreceptor degenerations. J Comp Neurol 464:1–16
40. Hwang YH, Kim S–WW, Kim YY, Na JH, Kim HK, Sohn YH (2012) Optic Nerve Head, Retinal Nerve Fiber Layer, and Macular Thickness Measurements in Young Patients with Retinitis Pigmentosa. Curr Eye Res 37:914–920
41. Walia S, Fishman GA, Edward DP, Lindeman M (2007) Retinal nerve fiber layer defects in RP patients. Invest Ophthalmol Vis Sci 48:4748–4752
42. Walia S, Fishman GA (2008) Retinal nerve fiber layer

analysis in RP patients using Fourier-domain OCT. Invest Ophthalmol Vis Sci 49:3525–3528
43. Oishi A, Otani A, Sasahara M, Kurimoto M, Nakamura H, Kojima H, Yoshimura N (2009) Retinal nerve fiber layer thickness in patients with retinitis pigmentosa. Eye 23:561–566
44. Jones BW, Pfeiffer RL, Ferrell WD, Watt CB, Marmor M, Marc RE (2016) Retinal remodeling in human retinitis pigmentosa. Exp Eye Res 150:149–165
45. García-Ayuso D, Di Pierdomenico J, Vidal-Sanz M, Villegas-Pérez MP (2019) Retinal ganglion cell death as a late remodeling effect of photoreceptor degeneration. Int J Mol Sci 20:1–16
46. Takagi S, Hirami Y, Takahashi M, Fujihara M, Mandai M, Miyakoshi C, Tomita G, Kurimoto Y (2018) Optical coherence tomography angiography in patients with retinitis pigmentosa who have normal visual acuity. Acta Ophthalmol 96:e636–e642
47. Cheng D, Wang Y, Huang S, Wu Q, Chen Q, Shen M, Lu F (2016) Macular Inner Retinal Layer Thickening and Outer Retinal Layer Damage Correlate With Visual Acuity During Remission in Behcet's Disease. Invest Ophthalmol Vis Sci 57:5470–5478
48. Schuerch K, Marsiglia M, Lee W, Tsang SH, Sparrow JR (2016) Multimodal imaging of disease-associated pigmentary changes in retinitis pigmentosa. In: Retina. Lippincott Williams and Wilkins, pp S147–S158
49. Li ZY, Possin DE, Milam AH (1995) Histopathology of bone spicule pigmentation in retinitis pigmentosa. Ophthalmology 102:805–816
50. Sodi A, Lenzetti C, Murro V, Caporossi O, Mucciolo DP, Bacherini D, Cipollini F, Passerini I, Virgili G, Rizzo S (2018) EDI-OCT evaluation of choroidal thickness in retinitis pigmentosa. Eur J Ophthalmol 28:52–57
51. Murakami Y, Funatsu J, Nakatake S, et al (2018) Relations among foveal blood flow, retinal-choroidal structure, and visual function in retinitis pigmentosa. Investig Ophthalmol Vis Sci 59:1134–1143
52. Balasopoulou A, Kokkinos P, Pagoulatos D, et al (2017) Symposium Recent advances and challenges in the management of retinoblastoma Globe - saving Treatments. BMC Ophthalmol 17:1
53. Kawano H, Sonoda S, Saito S, Terasaki H, Sakamoto T

(2017) CHOROIDAL STRUCTURE ALTERED by DEGENERATION of RETINA in EYES with RETINITIS PIGMENTOSA. Retina 37:2175–2182
54. Falsini B, Anselmi GM, Marangoni D, D'Esposito F, Fadda A, di Renzo A, Campos EC, Riva CE (2011) Subfoveal choroidal blood flow and central retinal function in retinitis pigmentosa. Investig Ophthalmol Vis Sci 52:1064–1069
55. Yu DY, Cringle SJ (2005) Retinal degeneration and local oxygen metabolism. Exp Eye Res 80:745–751
56. Korte GE, Reppucci V, Henkind P (1984) PRE destruction causes choriocapillary atrophy. Investig Ophthalmol Vis Sci 25:1135–1145
57. Neuhardt T, May CA, Wilsch C, Eichhorn M, Lütjen-Drecoll E (1999) Morphological changes of retinal pigment epithelium and choroid in rd- mice. Exp Eye Res 68:75–83
58. Saint-Geniez M, Kurihara T, Sekiyama E, Maldonado AE, D'Amore PA (2009) An essential role for RPE-derived soluble VEGF in the maintenance of the choriocapillaris. Proc Natl Acad Sci U S A 106:18751–6
59. ten Berge JC, Fazil Z, van den Born I, Wolfs RCW, Schreurs MWJ, Dik WA, Rothova A (2019) Intraocular cytokine profile and autoimmune reactions in retinitis pigmentosa, age-related macular degeneration, glaucoma and cataract. Acta Ophthalmol 97:185–192

Abstract

목적: 망막색소변성 환자에서 망막과 맥락막 미세구조의 변성 과정을 관찰하고자 한다

방법: 스펙트럼 영역 빛간섭단층촬영을 시행한 177명의 망막색소변성 환자와 같은 수의 건강한 대조군에서 단층연구를 시행하였다. 망막색소변성의 위중도는 내절타원영역의 온전한 정도를 기준으로 경도/중등도/진행된의 3단계로 구분하였다. 빛간섭단층촬영 영상에서 망막신경섬유층과 신경절세포-속얼기층을 수동으로 구획하였다. 이렇게 구해진 두 층의 두께를 중등도와 진행된 망막색소변성과 대조군에서 비교 분석하였다. 두 층의 망막두께, 시력, 시야 사이의 피어슨 상과계수를 계산하였다. 장기간 관찰연구에는 4년이상 기간의 빛간섭단층촬영 기록이 있는 69명의 망막색소변성 환자와 같은 수의 대조군 자료를 이용하였다. 망막과 맥락막의 각 층의 두께를 수동으로 구획하여 분석하였다. 망막색소상피 위축 넓이와 맥락막혈관지수 또한 분석하였다.

결과: 신경절세포-속얼기층 두께는 중등도 망막색소변성에서 대조군보다 두꺼웠지만 (P <0.001), 진행된 군에서는 중등도 군에서보다 얇았다. (P <0.001) 망막신경섬유층 두께는 중등도 군에서 정상보다 두꺼웠으며, 진행된 군에서 중등도 군보다 두꺼웠다. (모든 P <0.001) 신경절세포-속얼기층 두께는 나쁜 시력과 약한 양의 상관 관계를 보였다. 망막신경섬유층 두께는 나쁜 시력과 시야 위축과 양의 상관 관계가 있었다. 장기간 관찰 연구에서는, 중등도 군에서 신경절세포-속얼기층 (−1.38±1.49), 바깥세포층 (−1.05±1.39),

내절타원영역 (−0.94±1.54)에서, 진행된 군에서는 신경절세포−속얼기층과 망막신경섬유층에서 유의한 두께감소가 (평균±표준편차 ㎛/년) 관찰되었다. (모든 P < 0.01) 맥락막 두께는 −7.62 ~ −9.40 ㎛/년의 속도로 경도, 중등도 그리고 진행된 군에서 모두 통계적으로 유의하게 감소하였다. 망막색소상피 위축과 맥락막혈관지수 감소는 진행된 군에서 관찰되었다. 대조군에서는 아무 변화도 관찰되지 않았다. 결론: 단층연구를 통해서 망막색소변성에서 신경절세포−속얼기층과 망막신경섬유층을 포함하는 내층 망막이 시세포층에 비하여 장기간 보존되는 것을 발견할 수 있었다. 또한 망막 내층과 망막 기능의 관련성을 파악할 수 있었다. 장기간 관찰연구를 통해서는 바깥세포층과 신경절세포−속얼기층의 두께는 중등도와 진행된 망막색소변성에서 감소하였으며 망막신경섬유층 두께는 진행된 군에서만 감소하였다. 맥락막 두께는 모든 망막색소변성 군에서 감소하였다. 이에 더하여 망막색소상피 위축과 맥락막혈관지수 감소가 진행된 군에서 관찰되었다.